Spectrochimica Acta Part A: Molecular and Biomolecular Spectroscopy 274 (2022) 121071

Contents lists available at ScienceDirect

Spectrochimica Acta Part A: Molecular and Biomolecular Spectroscopy

journal homepage: www.elsevier.com/locate/saa

# Internal rotation analysis of the microwave and millimeter wave spectra of fluoral ($CF_3CHO$)

C. Bermudez [a,b,c,*], R.A. Motiyenko [a], C. Cabezas [b,d], V.V. Ilyushin [e,f], L. Margulès [a], Y. Endo [d], J.-C. Guillemin [g]

[a] Université de Lille, CNRS, UMR 8523 - PhLAM - Physique des Lasers Atomes et Molécules, Lille 59000, France
[b] Grupo de Astrofísica Molecular, Instituto de Física Fundamental (IFF-CSIC), C/ Serrano 121, 28006 Madrid, Spain
[c] Departamento de Química Física y Química Inorgánica, Facultad de Ciencias - I.U. CINQUIMA, Universidad de Valladolid, Paseo de Belén 7, Valladolid 47011, Spain
[d] Department of Applied Chemistry, Science Building II, National Yang Ming Chiao Tung University, 1001 Ta-Hsueh Rd., Hsinchu 300098, Taiwan
[e] Institute of Radio Astronomy of NASU, 4 Mystetstv St, Kharkiv 61002, Ukraine
[f] Quantum Radiophysics Department, V.N. Karazin Kharkiv National University, Svobody Square 4, 61022 Kharkiv, Ukraine
[g] Univ Rennes, Ecole Nationale Supérieure de Chimie de Rennes, CNRS, ISCR–UMR 6226, F-35000 Rennes, France

## HIGHLIGHTS

- Fluoral is a decomposition product of fluorinated compounds in the atmosphere.
- Fluoral has a very complex rotational spectrum due to the internal rotation motion.
- Fluoral has one of the highest coupling (ρ) between internal and overall rotations.
- Rho-axis-method implemented in RAM36 successfully treats species with high ρ.
- Methodological aspects must be considered to treat species with strong coupling.

## GRAPHICAL ABSTRACT

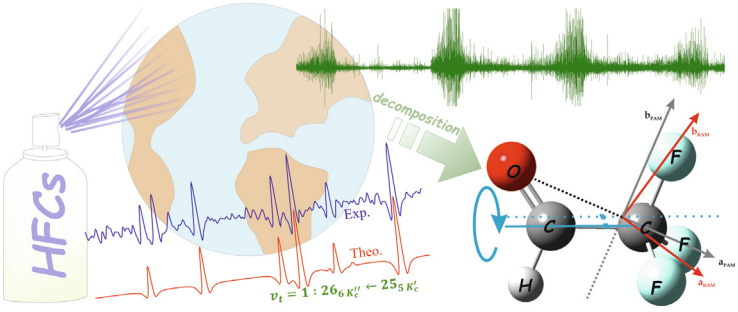


## ARTICLE INFO

*Article history:*
Received 7 December 2021
Received in revised form 9 February 2022
Accepted 20 February 2022
Available online 24 February 2022

*Keywords:*
Atmospheric
High resolution
Molecular spectroscopy
Rotational spectroscopy
Large amplitude motion
Fluorinated aldehydes

## ABSTRACT

The rotational spectrum (4–40 GHz and 50–330 GHz) has been measured and analyzed for trifluoroacetaldehyde, also known as fluoral ($CF_3CHO$), which is one of the degradation products of the fluorinated contaminants emitted into the atmosphere. The complexity of the spectroscopic analysis of this molecule arises from the strong coupling between the internal rotation motion of $CF_3$ group and the overall rotation of the molecule. The value obtained for its coupling constant (ρ = 0.91723481(49)) is comparable to the corresponding value of methanol ($CH_3OH$, ρ = 0.81), which is known for its complex spectrum. A total of 12,322 transitions of the ground, the first and second excited torsional states ($\Delta E_{1\upsilon t}$ = 62.0183(13) $cm^{-1}$; $\Delta E_{2\upsilon t}$ = 120.3315(13)$cm^{-1}$) with $J \leq 50$ were included in the analysis that was performed employing the rho-axis-method (RAM), and the RAM36 code. A fit within experimental error (root mean square deviation equals to 35 kHz) has been achieved for this dataset using 47 parameters of the RAM torsion-rotation Hamiltonian. In the course of the analysis, it became evident that for such high ρ value, as it is determined for fluoral, a larger than usual torsional basis set at the first diagonalization step of the two-step diagonalization procedure is required for achieving a fit within experimental error.


* Corresponding author.
*E-mail address:* celina.bermudez@uva.es (C. Bermudez).

https://doi.org/10.1016/j.saa.2022.121071
1386-1425/

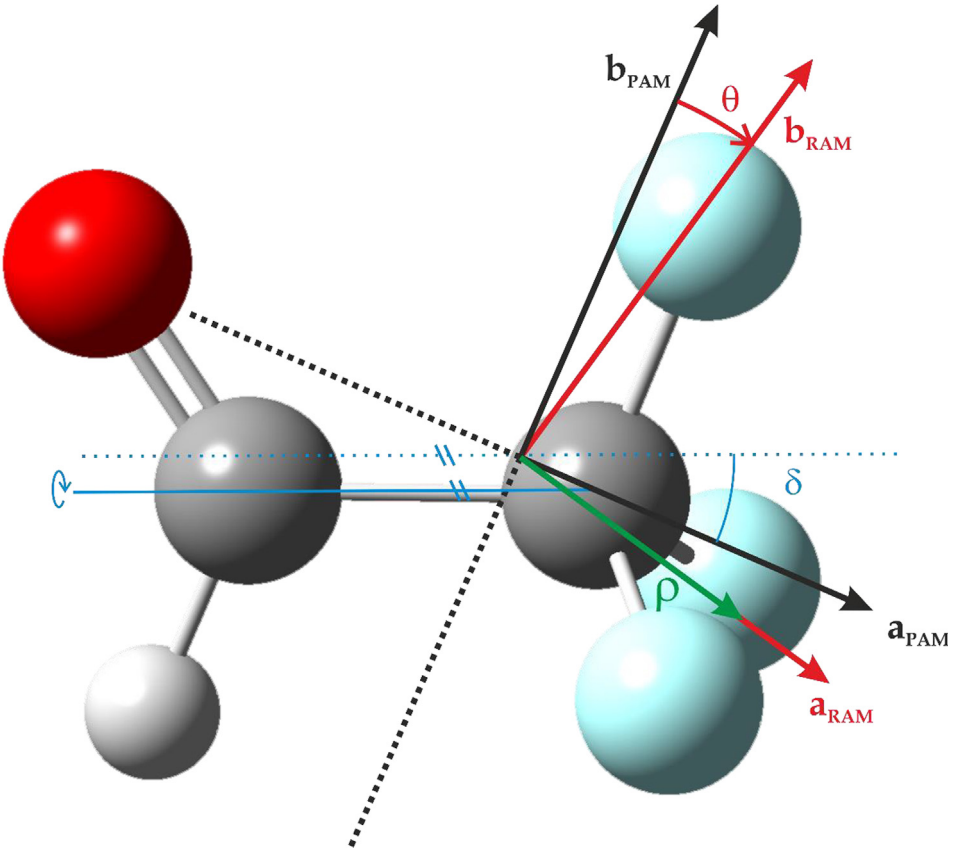


**Fig. 1.** Representation of the *ab initio* structure of the fluoral molecule. A comparison between the principal axis system and the rho-axis system is shown together with the $\rho$-vector and the significant angles of the axis frame.

## 1. Introduction

Recognition of the adverse impact of chlorofluorocarbons (CFCs) on stratospheric ozone prompted the substitution of the CFCs as refrigerants, cleaning solvents, foam-blowing agents, and aerosol propellants with environmentally more acceptable alternatives. Hydrochlorofluorocarbons (HCFCs), due to their similarity to CFCs in physicochemical properties, have been used as interim replacements for CFCs. However, HCFCs still contain chlorine; hence a virtual phase-out of HCFCs was scheduled by 2020 according to the updated Montreal Protocol [1]. Currently, hydrofluorocarbons (HFCs) have been used as acceptable alternatives to CFCs and HCFCs because they are "ozone friendly" and present short atmospheric lifetimes and relatively low global warming potentials [2]. However, there are some environmental hazards and health risks associated to HFCs since they are potent greenhouse gases and, thus, they would be harmful to climate.

HFCs have high volatility and very low solubility in water. Following their releases into the environment, these compounds reside in the atmosphere where they can undergo chemical degradation into different species. One of these degradation products is the trifluoroacetaldehyde ($CF_3CHO$), commonly known as fluoral. It is produced in the atmosphere by the degradation of some HFCs, and halo-olefins [2]. Atmospheric fluoral is decomposed in the troposphere by sunlight photolysis, or by its oxidation with the OH radical, with typical lifetimes of $\tau_{photol} > 27$ days and $\tau_{OH} \sim 26$ days [3]. Monitoring fluoral in the atmosphere can provide valuable information to understand the atmospheric chemistry of the HFCs, but it requires primarily the detailed knowledge of the intrinsic molecular properties of fluoral.

The literature on fluoral spectrum investigation is quite sparse. Although infrared and Raman spectra have been reported [4,5], to our knowledge the electronic spectrum remains unknown. Concerning the rotational spectrum of fluoral, the sole investigation published was carried out by Woods [6] in the 60's employing Stark-modulation spectroscopy up to 40 GHz. In this work, he described some interesting issues in the spectroscopic analysis of the internal rotation, caused by the intrinsic difficulties of the treatment of a heavy top molecule as fluoral ($CF_3CHO$), together with some deficiencies in the analysis. Compared to its homologue acetaldehyde ($CH_3CHO$), the substitution of a methyl group ($CH_3$–) by the trifluoro one ($CF_3$-) in fluoral leads to a significant increase of the mass of the top: the trifluoromethyl top is indeed heavier than the molecular frame (–CHO). Therefore, there is a strong coupling between the overall molecular rotation and the internal rotation of the top. The reported value of the coupling constant $\rho$ for fluoral is $\sim 0.9$ ($\rho_{max} = 1$) which is comparable to the $\rho$ value of molecules with elevated level of spectrum complexity such as methanol ($CH_3OH$, $\rho = 0.81$). In the present work, we present an analysis of the millimeter wave spectrum of fluoral employing a Hamiltonian based on the rho-axis method (hereafter RAM) in order to deal with some of the issues found in the previous analysis of fluoral.

## 2. Theoretical calculations

Fluoral (2,2,2-trifluoroacetaldehyde) is a quasi-planar molecule containing only two symmetric fluor atoms out of the plane (see Fig. 1). Therefore, it has a $C_s$ frame and a $C_{3v}$ top, and belongs to $G_6$ molecular symmetry group. The structure of fluoral was opti-

**Table 1**
Comparison of the current experimental results for fluoral with previous ones, theoretical *ab initio* ones and with those for the non-fluorinated homologue, acetaldehyde.

| Parameter[1] | This work | Literature[2] | *Ab initio*[3] | Acetaldehyde[4] | Units |
|---|---|---|---|---|---|
| $A_{PAM}$ | 5492.497 | 5490.170 | 5474.709 | 56799.135 | MHz |
| $B_{PAM}$ | 2983.908 | 2983.725 | 2978.699 | 10162.143 | MHz |
| $C_{PAM}$ | 2930.539 | 2935.920 | 2927.933 | 9089.229 | MHz |
| $A_{RAM}$ | 5377.365 | 5378.391 | 5337.368 | 56507.320 | MHz |
| $B_{RAM}$ | 3099.040 | 3095.504 | 3116.040 | 10453.957 | MHz |
| $C_{RAM}$ | 2930.539 | 2935.920 | 2927.933 | 9089.229 | MHz |
| $D_{ab}$ | −524.941 | −517.372 | −569.159 | −3677.525 | MHz |
| $\theta$ | −12.37 | −12.19 | −13.57 | −4.54 | ° |
| $\rho$ | 0.917 | 0.922 | 0.885 | 0.329 | – |
| $V_3$ | 284.740 | 318.5 | 329.780 | 407.598 | $cm^{-1}$ |
| $F$ | 55.848 | 62.783 | 53.934 | 226.855 | GHz |
| $s$ | 67.93 | 67.6 | 81.47 | 23.94 | – |
| $\mu_{aPAM}$ | [0.15][5] | 0.15(3) | 0.18 | 2.5160(43)[7] | D |
| $\mu_{bPAM}$ | [−1.64][5] | −1.64(5) | −1.71 | −1.0700(65)[7] | D |
| $\delta$ | 21.98 | 21.70 | 23.92 | 23.92 | ° |
| $\lambda_a$ | 0.927 | 0.929 | 0.914 | 0.914 | – |
| $\lambda_b$ | −0.374 | −0.370 | −0.405 | −0.405 | – |
| $I_\alpha$ | 88.56[6] | 89.321 | [89.321][5] | 3.23(6) | uÅ |

[1] *A,B,C* with corresponding indices are the rotational constants of the molecule in PAM and RAM axis systems. $\theta$ is the angle between PAM and RAM axis frames (see Fig. 1). $V_3$ is the leading term in the cosines series expansion of the internal rotation barrier $V(\alpha)=\frac{V_3}{2}(1-\cos 3\alpha)+\frac{V_6}{2}(1-\cos 6\alpha)\cdots$ with $\alpha$ being the rotation angle of the $CF_3$ (fluoral) or $CH_3$ (acetaldehyde) top with respect to –CHO frame. $F$ is the internal rotation constant $F=\frac{\hbar^2}{2rI_\alpha}$ where $r=1-\sum_g \lambda_g^2\frac{I_\alpha}{I_g}$; $I_\alpha$ is the moment of inertia of the $CF_3/CH_3$ top; $I_g$ ($g$ = *a,b,c*), the moments of inertia of the molecule in the principal axis system, and $\lambda_g^2(g=a,b,c)$ represent the direction cosines of the internal rotation axis of the top and the principal axis (e.g. see Fig. 1, $\lambda_a=\cos\delta$). $s$ is a reduced torsional barrier height calculated as $s=4V_3/9F$ [27]. The $\rho$ vector is represented in green in the Fig. 1. Its coordinates are calculated using the following expression: $\rho_g=\frac{I_g}{\lambda_g I_\alpha}$. $\mu_g$ ($g$ = *a,b*), the dipole moment projection along the principal axes system ($\mu_c$ = 0 for fluoral and acetaldehyde).

[2] From Woods [6].

[3] Estimated at MP2/aug-cc-pVTZ with Gaussian 09 (Revision E.01).

[4] Acetaldehyde was taken for comparison since it has the same molecular frame –CHO to which a much lighter $CH_3$ top is attached (in contrast to the heavy $CF_3$ top in fluoral). Data for acetaldehyde were taken from Smirnov et al. [26].

[5] Fixed to the value of Woods [6]. The relative signs of the dipole moment components were determined from our ab initio results.

[6] Average of the two $I_\alpha$ values recalculated from $F$ and $\rho$ parameters.

[7] Values estimated in ref. Kleiner et al. [28].

mized using quantum chemical calculations at MP2/aug-cc-pVTZ level. All these calculations were performed with Gaussian 09 Revision E.01.

Based on the minimum energy structure found *ab initio*, we have calculated some relevant parameters for the internal rotation analysis which are collected in Table 1. Among them, there are the estimated values for the rotational constants *A,B,C*, not only in the principal axis system, but also in the $\rho$ axis system. The latter axis system is employed in rho-axis-method (RAM) to analyze molecules with internal rotation motions. As it is shown in Fig. 1, in the $\rho$ axis system, $z$ axis becomes parallel to the $\rho$ vector. The direction and the module of this $\rho$ vector, as well as the internal rotation constant $F$, are calculated based on the direction cosines of the internal rotation axis of the top (in light blue in the figure) with respect to the principal axes. See literature [7,8], and caption of Table 1 for further information about these values. Furthermore, we estimated the internal rotation energy barrier, $V_3$, to be ~329 $cm^{-1}$ by scanning the F-C-C-O torsional angle at MP2/aug-cc-pVTZ level of theory.

The energy of the torsional mode of fluoral is estimated to be 65.5 $cm^{-1}$ under the anharmonic correction (MP2/aug-cc-pVTZ), relatively close to the value provided in the literature: ~55 $cm^{-1}$ [4]. According to this calculation, the displacement vectors of this vibrational mode are centered in the aldehyde part of the molecule (the conventional frame), instead of being centered in the trifluoro methyl group (the standard top for the internal rotation). Woods [6], based on the low value of the reduced moment $r$ (see caption Table 1), roughly interpreted that it is the aldehyde light frame who rotates along the fixed heavy trifluoromethyl top, which is in agreement with the displacement vectors found in our calculations.

## 3. Experimental details

The experimental measurements were conducted in two different stages: the low frequency measurements (4–40 GHz) were performed using the Balle-Flygare narrow-band type Fourier-transform microwave (FTMW) spectrometer at the National Yang Ming Chiao Tung University in Taiwan [9], and the millimeter wave spectrum (50–330 GHz) was recorded at the University of Lille.

Fluoral was found as the main product in the reactions aimed to characterize the Criegee intermediate, trifluoroacetaldehyde oxide ($CF_3CHOO$), using 1,1,1-trifluoro-2,2-diiodoethane ($CF_3CHI_2$) as a potential precursor. The 1,1,1-trifluoro-2,2-diiodoethane was synthesized in a two-step reaction starting from 2,2,2-trifluoroethylamine hydrochloride ($CF_3CH_2NH_3^+Cl^-$) and sodium nitrite ($NaNO_2$) in water to form the diazo derivative ($CF_3CHN_2$) [10], which was extracted with diethyl ether and then treated with iodine until a weak coloration of the solution. Purification was carried out by distillation under vacuum at a pressure of 0.1 mbar and selective trapping at −40 °C. Yield: 52%.

The mixture of gases, 2% $O_2$ and 98% Ar, with the total pressure of 1.5 atm was passed through a container filled with liquid 1,1,1-trifluoro-2,2-diiodoethane in order to introduce the precursor molecules with a sufficient partial pressure. The gas mixture (1,1,1-trifluoro-2,2-diiodoethane, $O_2$ and Ar) was flowed through a pulsed-solenoid valve that is accommodated in the backside of one of the cavity mirrors, and aligned parallel to the optical axis

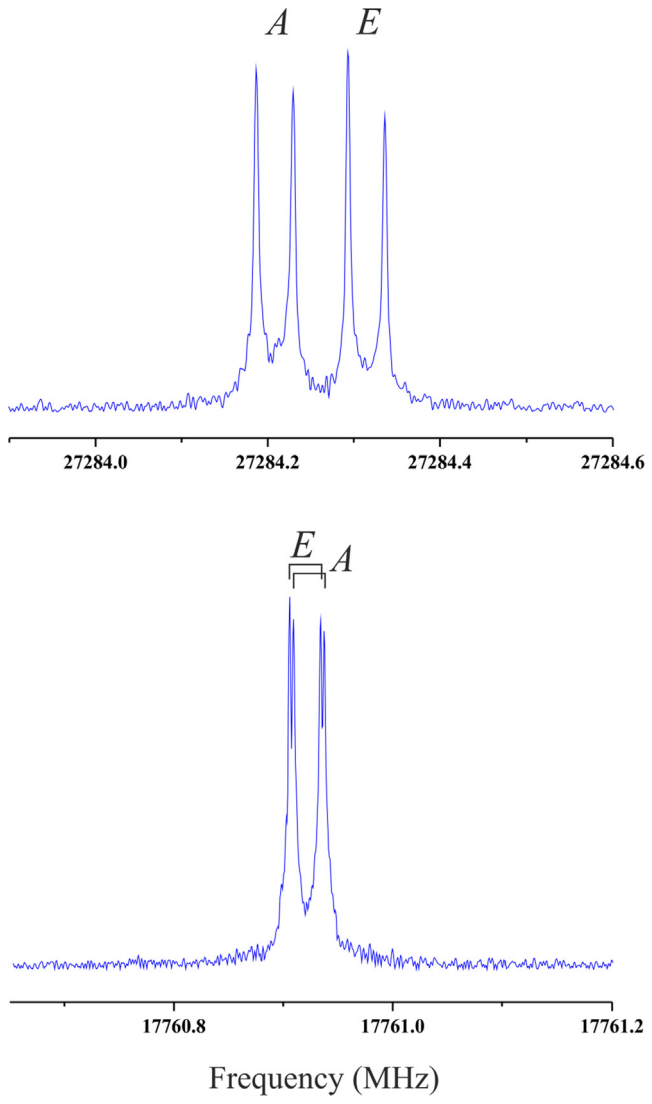


**Fig. 2.** The FTMW spectra of the $5_{05}$–$4_{04}$ (upper panel) and $3_{21}$–$2_{20}$ (lower panel) rotational transitions of fluoral in the ground torsional state. The spectra were achieved by 50-shots of accumulation. Each of the *A*-*E* observed lines is split into two Doppler components because the microwave radiation in the Fabry-Pérot cavity propagates parallel and antiparallel to the unidirectional molecular beam.

of the resonator. A pulsed voltage of 800 V and 450 μs of duration was applied between the two stainless steel electrodes attached at the exit of the nozzle of the pulsed valve [11], creating an electric discharge synchronized with the gas expansion. The resulting products generated in the discharge were supersonically expanded, rapidly cooled to a rotational temperature of ~2.5 K between the two mirrors of the Fabry–Pérot resonator, and then probed by Fourier-transform microwave spectroscopy. MW-MW double-resonance techniques [12] were also used for observing pure rotational transitions and confirming the assignments of those observed by FTMW spectroscopy. Although such experiments were performed to identify a Criegee intermediate, only the spectrum of the fluoral was observed.

For the millimeterwave experiments recorded at the University of Lille, fluoral was synthesized starting from the corresponding commercially available hemiacetal. Dropwise addition of trifluoroacetaldehyde ethyl hemiacetal (7.13 g, 50 mmol) to polyphosphoric acid (15 mL) heated to 150–180 °C and condensation of the gaseous flow in a cold trap (77 K) led to fluoral in a 90% yield [13]. The resulting product was flowing continuously in the spectrometer at room temperature, maintaining a pressure of 0.028 mbar.

The millimeter wave spectrometer of Lille is described in the literature [14]. In this experiment, we employed the fast-scan mode (up to 50 μs/point of frequency switching rate). This equipment is based on mixing the filtered signal of an Agilent E8257 synthesizer (up to 20 GHz) with that of a direct digital synthesizer DDS (AD9915). After filtering with a YIG bandpass filter, the frequency range of the signal is in the $K_u$ band. The fast scan mode is obtained by sweeping the DDS within the filter bandwidth of 25–40 MHz. The output signal in the $K_u$ band is then used as input for a multiplication chain that gets up to 330 GHz. In case of the 50–75 GHz frequency range, the filtered signal was used as input for a Millitech active multiplier (x4). To obtain higher frequencies, an active sextupler AMC-10 (VDI) that covers the W-band range (75–110 GHz) was employed. This signal can be sent directly to the sample cell, or it can be used as input for a second multiplication step. This second step consists of a passive Schottky multiplication using a doubler (150–220 GHz), or a tripler (225–330 GHz). In any of these cases, the detection was carried out employing a series of Schottky diode zero biased detectors from VDI: WR15ZBD (50–75 GHz), WR10ZBD (75–110 GHz), WR5.1ZBD (150–220 GHz), and WR3.4ZBD (225–330 GHz).

## 4. Results

Using the rotational constants reported by Woods [6], the rotational transitions for fluoral up to 40 GHz were predicted with the XIAM program [15], and most lines were observed very close to the expected frequencies. A total of 149 pure rotational transitions including *a*- and *b*-type transitions were observed using the FTMW spectrometer (see Fig. 2 where observed *A* - *E* torsional splittings

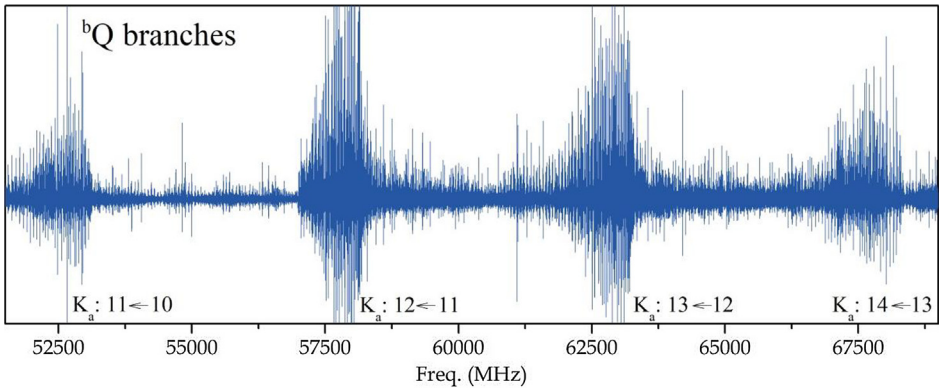


**Fig. 3.** Millimeter wave spectrum of fluoral demonstrating a prominent *b*-type *Q* branch structure.

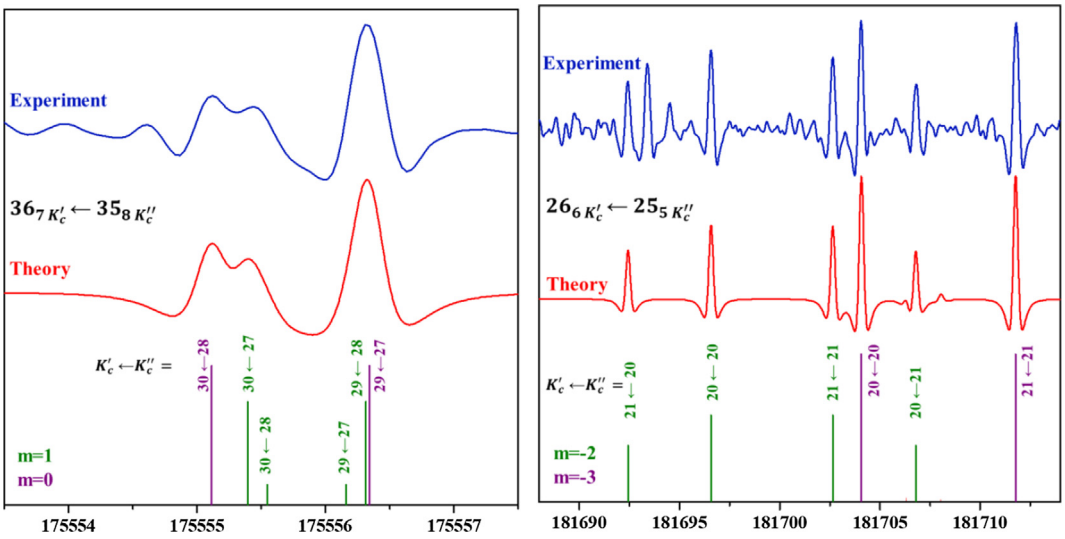


**Fig. 4.** Examples of fluoral transitions where the standard selection rules for an asymmetric molecule with b-type dipole moment are not respected. In red, the predicted transitions in a stick mode with the simulation of the profile (lower trace). The simulation profile is calculated using Lorentzian line shapes, HWHM (Half Width Half Maximum) of 0.33 MHz and the line-strength predicted by the fit. In blue, the experimental spectrum of fluoral is given (upper trace). The figure on the left corresponds to a transition of the ground state, and on the right, to the first torsional excited state. (For interpretation of the references to colour in this figure legend, the reader is referred to the web version of this article.)

are illustrated for two example transitions). After several unsatisfactory attempts to analyze the observed frequency transitions with the XIAM program [15], we switched to the RAM36 program [16,17], which is believed to be more suitable for molecules with a strong coupling between internal and overall rotations ($\rho \approx 0.9$ in fluoral).

In the millimeter wave range several features characteristic of a b-type spectrum of a quasi-prolate rotor were observed; see, for instance, in Fig. 3 the pattern of the $^{b}$Q branches. Using the Loomis-Wood plots, we could assign low $J$ and $K_a$ $^{b}$R-branch transitions, of the ground state and of the first torsional excited state. Once we have included in the fit transitions up to $K_a$ = 10 for the ground state and up to $K_a$ = 3 for the first excited torsional state, we encountered a problem with including higher $K_a$ transitions in the fit since they were not well predicted by the model. Whereas using the Loomis-Woods plots we were able to identify the transition series, the model could not fit them satisfactorily, even involving additional terms of a rather high order. Investigation into this problem revealed a necessity to enlarge the torsional basis set for the first diagonalization step implemented in the RAM36 code. The RAM36 code uses the two-step diagonalization procedure of Herbst et al. [18]. In the first step a set of torsional calculations is performed with a relatively large torsional basis set of the form exp[i(3 $l$ + σ)α] for σ = 0, 1 ($m$ = 3 $l$ + σ). The size of the basis set in the first step can be varied by choosing a value for *ktronc* (where $l$ runs over the values from -*ktronc* to +*ktronc*). In this step usually only the main pure torsional terms and $K$ dependent torsion-rotation coupling due to ρ parameter are taken into account. No $J$ dependent terms are allowed at the first diagonalization step. In the second step, a reduced number of torsional basis set functions is used (*nvt*), which is obtained by discarding all but the lowest *nvt* torsional eigenfunctions of the first step. In the second step, a separate matrix of dimension (2 $J$ + 1) × *nvt* is built for each symmetry and $J$ values, and all desired rotation and torsion-rotation effects are taken into account. In the current study of fluoral we were forced to use slightly larger (*ktronc* = 15) as usual (*ktronc* = 10) torsional basis set at the first diagonalization step (see Discussion section for further details). This basis set enlargement had a very positive effect on the fit, allowing us in the end to get a fit within experimental error for the dataset treated, and to expand our assignments to transitions with much higher $K_a$ quantum numbers.

Some anomalies in intensity predictions for a number of $^{b}R$ and $^{b}Q$ series of transitions where also found. It was expected that series of transitions with standard asymmetric rotor $b$-type dipole moment selection rules will be dominating the spectrum. At some point, we noticed that moving up to the next $K_a$ in our assignment process brings us to the dominating $J$-series with somewhat different selection rules for $\Delta K_c$, which do not follow $b$-type dipole moment selection rules ($\Delta K_a$ = ±1, but $\Delta K_c$ was not always equal to ±1 as it is expected for $b$-type transitions). Moreover, sometimes this alteration in $\Delta K_c$ selection rule happens within one $J$-series of $\Delta K_a$ = +1 or $\Delta K_a$ = −1 transitions (i.e. large intensity at two adjacent $J$ values in the series of lines may correspond to two different selection rules for $\Delta K_c$). This situation was mainly observed for the millimeter wave spectrum. For the ground torsional state, it starts at somewhat higher $K_a$ values than for the excited torsional states. Only few "unexpected" transitions were observed in the microwave region, in particular, some b-type transitions with $\Delta K_c$ = ±3, and, nominally, c-type transitions with $\Delta K_c$ = 0, ±2. As it can be seen in Fig. 4, some transitions were split into transitions with $\Delta K_c$ that could range from 0 to ±3, including the 0, ±2 values, which are not expected for a $b$-type transition. A detailed discussion of why $K_c$ labels may not obey mathematically well-defined selection rules in molecules with large amplitude torsional motion, and how the nominal $a$-, $b$-, and $c$-type character of transitions may not coincide with the direction of the dipole moment component, actually responsible for the major contribution to the transition moment matrix element, can be found in the work of Hougen et al. [19], where the case of acetaldehyde is considered. Nominally "forbidden" $c$-type transitions were already reported for some other molecules with torsional large amplitude motion (see for example corresponding discussion for the methyl formate molecule in [20]). But, in fact, the root of our problems lies in the tight clustering of the fluoral energy levels, which lead to degenerate within machine round-off error pairs of levels, and the peculiarities of the energy labeling scheme implemented in RAM36. For higher $K_a$ values this clustering within machine round-off error starts at lower $J$ values. Of course, if a pair of levels is degenerated to within machine round-off error, then the eigenvectors returned by the

**Table 2**
Molecular parameters of fluoral obtained with the RAM36 program from the $v_t$ = 0,1,2 dataset fit.

| Parameter | Operator[a] | Order $n_{t,r}$[b] | Value[c] | Units |
|---|---|---|---|---|
| $A_{RAM}$ | $J_a^2$ | $2_{0,2}$ | 5377.3645(31) | MHz |
| $B_{RAM}$ | $J_b^2$ | $2_{0,2}$ | 3099.0398(31) | MHz |
| $C_{RAM}$ | $J_c^2$ | $2_{0,2}$ | 2930.53868(26) | MHz |
| $D_{ab}$ | $\left\{J_a^2, J_b^2\right\}$ | $2_{0,2}$ | −524.9412(70) | MHz |
| $\rho$ | $p_\alpha J_a$ | $2_{1,1}$ | 0.91723481(49) | – |
| $V_3$ | $½(1-\cos 3\alpha)$ | $2_{2,0}$ | 284.7397(26) | $cm^{-1}$ |
| F | $p_\alpha^2$ | $2_{2,0}$ | 1.862885(18) | $cm^{-1}$ |
| $\Delta_J$ | $-J^4$ | $4_{0,4}$ | 0.60073(15) | kHz |
| $\Delta_{JK}$ | $-J^2 J_a^2$ | $4_{0,4}$ | −38.086(76) | kHz |
| $\Delta_K$ | $-J_a^4$ | $4_{0,4}$ | 489.0(24) | kHz |
| $\delta_J$ | $-2J^2\left(J_b^2 - J_c^2\right)$ | $4_{0,4}$ | 0.0639102(70) | kHz |
| $\delta_K$ | $-\{J_a^2, \left(J_b^2 - J_c^2\right)\}$ | $4_{0,4}$ | 11.86(12) | kHz |
| $D_{abJ}$ | $½J^2\left\{J_a^2, J_b^2\right\}$ | $4_{0,4}$ | 2.0211(18) | kHz |
| $\rho_J$ | $p_\alpha J_a J^2$ | $4_{1,3}$ | −0.063905(97) | MHz |
| $\rho_K$ | $p_\alpha J_a^3$ | $4_{1,3}$ | 1.0263(53) | MHz |
| $\rho_{bc}$ | $½p_\alpha\left\{J_a, \left(J_b^2 - J_c^2\right)\right\}$ | $4_{1,3}$ | 0.05378(72) | MHz |
| $V_{3J}$ | $J^2(1-\cos 3\alpha)$ | $4_{2,2}$ | 9.4440(22) | MHz |
| $V_{3K}$ | $J_a^2(1-\cos 3\alpha)$ | $4_{2,2}$ | −4.1186(59) | MHz |
| $V_{3bc}$ | $\left(J_b^2 - J_c^2\right)(1-\cos 3\alpha)$ | $4_{2,2}$ | 1.757(29) | MHz |
| $V_{3ab}$ | $½\{J_a, J_b\}(1-\cos 3\alpha)$ | $4_{2,2}$ | −29.200(16) | MHz |
| $D_{3ac}$ | $½\{J_a, J_c\}\sin 3\alpha$ | $4_{2,2}$ | 10.885(18) | MHz |
| $D_{3bc}$ | $½\{J_b, J_c\}\sin 3\alpha$ | $4_{2,2}$ | 7.48(11) | MHz |
| $F_J$ | $p_\alpha^2 J^2$ | $4_{2,2}$ | 0.020841(31) | MHz |
| $F_{bc}$ | $p_\alpha^2\left(J_b^2 - J_c^2\right)$ | $4_{2,2}$ | −0.03004(56) | MHz |
| $\rho_m$ | $p_\alpha^3 J_a$ | $4_{3,1}$ | −1.1378(62) | MHz |
| $V_6$ | $½(1-\cos 6\alpha)$ | $4_{4,0}$ | −8.0374(39) | $cm^{-1}$ |
| $F_m$ | $p_\alpha^4$ | $4_{4,0}$ | 0.6048(34) | MHz |
| $\Phi_J$ | $J^6$ | $6_{0,6}$ | 0.0002111(52) | Hz |
| $\Phi_{KJ}$ | $J^2 J_a^4$ | $6_{0,6}$ | 2.775(99) | Hz |
| $\rho_{JK}$ | $p_\alpha J_a^3 J^2$ | $6_{1,5}$ | −3.87(11) | Hz |
| $V_{3JJ}$ | $J^4(1-\cos 3\alpha)$ | $6_{2,4}$ | −0.05218(32) | kHz |
| $V_{3abK}$ | $½\left\{J_a^3, J_b\right\}(1-\cos 3\alpha)$ | $6_{2,4}$ | 0.744(14) | kHz |
| $V_{3b2c2}$ | $½\left\{J_b^2, J_c^2\right\}\cos 3\alpha$ | $6_{2,4}$ | −0.15559(95) | kHz |
| $D_{3bcbc}$ | $½\left(\left\{J_b^3, J_c\right\} - \left\{J_b, J_c^3\right\}\right)\sin 3\alpha$ | $6_{2,4}$ | 0.05606(41) | kHz |
| $D_{3acK}$ | $½\left\{J_a^3, J_c\right\}\sin 3\alpha$ | $6_{2,4}$ | 0.406(16) | kHz |
| $V_{6J}$ | $J^2(1-\cos 6\alpha)$ | $6_{4,2}$ | 0.1925(11) | MHz |
| $V_{6K}$ | $J_a^2(1-\cos 6\alpha)$ | $6_{4,2}$ | −0.8764(32) | MHz |
| $V_{6bc}$ | $\left(J_b^2 - J_c^2\right)(1-\cos 6\alpha)$ | $6_{4,2}$ | −1.486(35) | MHz |
| $D_{6ac}$ | $½\{J_a, J_c\}\sin 6\alpha$ | $6_{4,2}$ | −1.046(17) | MHz |
| $D_{6bc}$ | $½\{J_b, J_c\}\sin 6\alpha$ | $6_{4,2}$ | 3.299(58) | MHz |
| $F_{mJ}$ | $p_\alpha^4 J^2$ | $6_{4,2}$ | 1.1265(89) | Hz |
| $F_{mm}$ | $p_\alpha^6$ | $6_{6,0}$ | −0.0296(16) | Hz |
| $V_{6JJ}$ | $J^4(1-\cos 6\alpha)$ | $8_{4,4}$ | 0.00412(13) | kHz |
| $V_{6JK}$ | $J^2 J_a^2(1-\cos 6\alpha)$ | $8_{4,4}$ | −0.0343(10) | kHz |
| $D_{6acJ}$ | $½J^2\{J_a, J_c\}\sin 6\alpha$ | $8_{4,4}$ | −0.0735(22) | kHz |
| $D_{6bcJ}$ | $½J^2\{J_b, J_c\}\sin 6\alpha$ | $8_{4,4}$ | −0.01153(32) | kHz |
| $D_{6bcK}$ | $½\{J_a^2, J_b, J_c\}\sin 6\alpha$ | $8_{4,4}$ | 0.428(16) | kHz |
| $\mu_{aRAM}$[d] | | | [−0.205] | D |
| $\mu_{bRAM}$[d] | | | [−1.634] | D |

[a] Operator corresponding to the parameter following the Hamiltonian expression incorporated in the RAM36 code (see results section).
[b] Order of the operator n = t + r, where n is the total order of the operator, t is the order of the torsional part and r is the order of the rotational part, respectively.
[c] Statistical uncertainties are shown as one standard uncertainty in the last two digits.
[d] Dipole moments in the rho axis frame fixed in the fit to the values derived from the principal axis values of Woods et al. [6].

diagonalization algorithm will be random linear combinations of the "true" eigenvectors. At the same time, the $K_a$, $K_c$ labeling in the RAM36 code is based on energy ordering of the levels in a particular torsional state. Thus, for a degenerate pair of levels in fluoral, we have a situation when eigenvectors properties, which are crucial for calculating transition intensity, may be randomly redistributed between two levels with the same $K_a$ but different $K_c$ values. As consequence, we get a situation when $\Delta K_a$ = ±1 selection rule is obeyed whereas $\Delta K_c$ selection rule may vary even within one $J$-series of lines. Namely, due to such type problems, the spectrum predictions implemented in the RAM36 code do not rely on any $\Delta K_a$, $\Delta K_c$ selection rules. The program calculates all possible

transition frequencies and intensities allowed by symmetry for a given pair of upper and lower state $J$ values, and displays all transitions with intensities above a user-set cutoff. Thus, there are no "missing" lines in the predictions due to the labeling issues discussed above.

The complete set of parameters included in the final analysis is presented in Table 2, along with the operators associated and the orders of these operators (we employed the ordering scheme of Nakagawa et al. [21]). These parameters give rise to a Hamiltonian model which is able to fit 12,322 transitions, that includes the $R$ and $Q$ type transitions of the ground, first and second excited torsional states up to $J$ = 50 and $K_a$ = 28, with the rms deviation of 35 kHz (corresponding to weighted rms deviation of 0.69). Table 1 gives a comparison between the main parameters obtained in the present fit with those from the literature and calculated *ab initio* as well as with parameters of the non-fluorinated homologue of fluoral, acetaldehyde. The selection of the parameters included in the final Hamiltonian model was not straightforward due to the correlation problems appearing for a number of high order Hamiltonian terms. Some high correlations remain evident even in the final fit involving mainly the following parameters: $F_m - \rho_m$, $F_m - \rho_K$, $\rho_m - \rho_K$, $\rho_K - \Delta_K$. Removing one of those parameters from our model was not an option because this led to a significant increase in the weighted rms deviation of the fit. Here, it should be noted that a spectrum of the fundamental torsional band of fluoral will eventually be necessary to stabilize and properly constrain the pure torsional parameters in the Hamiltonian (like $F$, $V_3$, $V_6$ as well as $F_m$, $\rho_m$). For the moment such parameters are determined here only very indirectly from rotational intervals within each torsional state and this, in particular, is the cause of the correlation problems encountered in our study.

## 5. Discussion

To our knowledge fluoral represents the case with the highest coupling between internal and overall rotations in a molecule studied so far using high resolution microwave spectroscopy ($\rho \approx 0.92$, see Table 1). The closest by $\rho$ value case to which fluoral may be compared is triply deuterated methanol $CD_3OH$ with $\rho \approx 0.89$ [22]. If we consider the molecules with heavy $CF_3$ internal top, then fluoral may be compared with trifluoropropene ($CF_3$-$CHCH_2$, $\rho \approx 0.81$) [23] and trifluoroacetic acid ($CF_3COOH$, $\rho \approx 0.67$) [24]. Here, it is interesting to compare A-E splittings observed in fluoral with trifluoroacetic acid spectra. In trifluoropropene, the barrier height is rather high ($V_3 \approx 653$ cm$^{-1}$), and torsional splittings are observed only in the second excited torsional state [23], which is not surprising in view of the heavy $CF_3$ top. In trifluoroacetic acid, the barrier height ($V_3 \approx 242$ cm$^{-1}$) is lower than in fluoral ($V_3 \approx 285$ cm$^{-1}$), but the torsional splittings in its rotational spectrum start to be resolvable by millimeter wave spectroscopy only in the third excited torsional state[24]. In fluoral, torsional splittings in the rotational spectrum are resolvable already in the ground torsional state demonstrating significant impact of much higher coupling between internal and overall rotations in this molecule ($\rho \approx 0.92$ in $CF_3CHO$ versus $\rho \approx 0.67$ in $CF_3COOH$).

One of the issues which posed, somewhat unexpectedly, a problem in the course of the fluoral spectrum analysis was the size of the torsional basis set at the first diagonalization step of the two-step diagonalization procedure [18] implemented in RAM36. Traditionally, starting from the first work of Herbst et al. [18], where this procedure was proposed, the formally infinite matrix of the first diagonalization step was truncated to 21 × 21 matrix (*ktronc* = 10), and it was believed that this size was enough to ensure the needed accuracy in the energies of the lowest torsional states [18]. Therefore, this truncation level was adopted further in many studies of molecular spectra using the RAM approach (see for example corresponding studies of methanol [25], acetaldehyde [26], acetic acid [17], etc.). In the case of fluoral, it appeared that we need to enlarge the torsional basis set at the first diagonalization step. To get a better understanding what is happening in the case of fluoral, let's consider the free rotor energy expression $E(m, K) = F(m\text{-}\rho K)^2$ in a zero barrier approximation for the cases of (a) acetic acid, (b) acetaldehyde, and (c) fluoral (see Fig. 5). Likewise, we focus on A-type levels ($\sigma$ = 0, in the basis set expression: exp[i(3 $l$ + $\sigma$)$\alpha$]) , and we would like to truncate the torsional basis set at $|m|$ = 18 (*ktronc* = 6). Thus, we are looking whether excluding of $|m|$ = 21 states from consideration at the first diagonalization step may be of importance for the second diagonalization step, where we keep *nvt* = 9 lowest torsional states for each considered $K$ value. In the

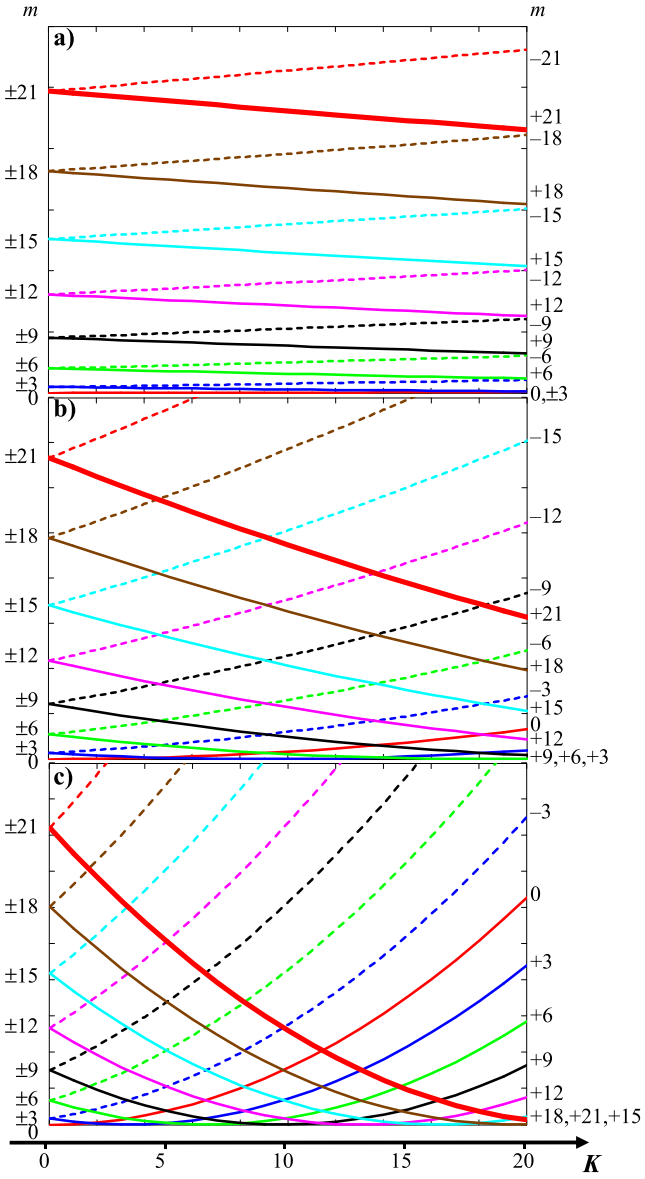


**Fig. 5.** Free rotor $m$ states and their reordering with $K$ quantum number due to torsion-rotation coupling. $E(m, K) = F(m\text{-}\rho K)^2$ energies are simulated for a) acetic acid like molecule ($F$ = 5.6 cm$^{-1}$, $\rho$ = 0.07); b) acetaldehyde like molecule ($F$ = 7.56 cm$^{-1}$, $\rho$ = 0.33); and c) fluoral like molecule ($F$ = 1.86 cm$^{-1}$, $\rho$ = 0.92). Dashed/solid lines correspond to negative/positive $m$ values, respectively. Free rotor $m$ quantum numbers are given at the left and at the right of the plots to illustrate the reordering. Note that the free rotor energies are given at different scales for a), b), c) plots to make more evident different extent of $m$ state reordering with $K$.

case of acetic acid, where $\rho$ is quite small ($\rho \approx 0.07$), there is no alteration in the energy order of different $m$ states between $K = 0$ and $K = 20$ (see Fig. 5a). It is evident that neither for $K = 0$, nor for $K = 20$, the $|m| = 21$ states will not appear among the $nvt = 9$ lowest, and thus truncation at $|m| = 18$ will not affect directly the second diagonalization step. In the case of acetaldehyde (see Fig. 5b), the $\rho$ value is bigger ($\rho \approx 0.33$), and the energy order of different $m$ states is now changing with $K$ value, but, still, neither for $K = 0$, nor for $K = 20$, the $|m| = 21$ states will not appear among the $nvt = 9$ lowest. The situation changes dramatically for fluoral where $\rho \approx 0.92$. Due to the strong torsion-rotation coupling in fluoral, the $m = 21$ state will be the second by energy at $K = 20$ (see Fig. 5c). Thus, if we would like to keep $nvt = 9$ lowest states for $K = 20$, it is not a good idea to exclude $|m| = 21$ states from consideration by truncating our first diagonalization step basis set at $|m| = 18$ ($ktronc = 6$). Therefore, in the case of $\rho \approx 0.92$, we need to increase our truncation limit to take into consideration a number of higher $m$ states above $|m| = 18$. Certainly, presence of potential barrier hindering internal rotation modifies the energy ordering in comparison with the simplified barrier free example considered here (the torsional energies are known to be oscillatory functions with period three in a variable $\rho K$ [27]), but $V_3$ barrier does not cancel energy reordering of $m$ states with $K$ value due to torsion-rotation coupling. It was found empirically that for the considered range of $K$ values in the case of fluoral, which possesses very high $\rho$ value of $\sim 0.92$, we need to enlarge torsional basis set of the first diagonalization step by a factor of 1.5 (from $ktronc = 10$ to $ktronc = 15$) to account for reordering of torsional $m$ states with $K$ and get a fit within experimental error.

## 6. Conclusion

Fluoral is a molecule of atmospheric interest with a complex rotational spectrum due to its internal rotation motion. Combination of the heavy $CF_3$ top with the relatively light CHO frame results in a strong coupling between the internal rotation and the overall rotation of the molecule, which is characterized by one of the largest ρ value studied so far with the microwave spectroscopy ($\rho$ = 0.91723481(49)). The microwave and millimeter wave spectrum analysis of fluoral was performed using the rho-axis-method and the RAM36 code. A total of 12,322 transitions of the ground, first and second excited torsional states, which, due to clustering and occasional blending, correspond to 9342 measured line frequencies, were involved in the analysis of the fluoral spectrum and the fit within experimental error (weighted root mean square deviation 0.69) has been achieved for this dataset using 47 parameters. The successful analysis required a larger than usual torsional basis set at the first diagonalization step of the two-step diagonalization procedure [18], which is a consequence of the very high $\rho$ value in fluoral.

## CRediT authorship contribution statement

**C. Bermudez:** Formal analysis, Investigation, Visualization, Writing – original draft, Writing – review & editing. **R. Motiyenko:** Conceptualization, Supervision, Formal analysis, Investigation. **C. Cabezas:** Investigation, Writing – original draft. **V. Ilyushin:** Formal analysis, Methodology, Validation, Writing – review & editing. **L. Margules:** Conceptualization, Supervision. **J.-C. Guillemin:** Investigation, Chemical synthesis, Writing – review & editing.

## Declaration of Competing Interest

The authors declare that they have no known competing financial interests or personal relationships that could have appeared to influence the work reported in this paper.

## Acknowledgments

This research was supported by the National French Programme "ANR Labex CaPPA" through the PIA under contract ANR-11-LABX-0005-01, by the contract CPER CLIMIBIO, by the Ministry of Science and Technology of Taiwan under Grant Nos MOST 104-2113-M-009-020 (Y.E.), and by MOST 105-2811-M-009-026 (C.C.). J.-C.G. thanks the Centre National d'Etudes Spatiales (CNES) for financial support.

## References

[1] A.G. Berends, C.G.d. Rooij, S. Shin-ya, R.S. Thompson, Biodegradation and ecotoxicity of HFCs and HCFCs, Arch. Environ. Contam. Toxicol. 36 (2) (1999) 146–151, https://doi.org/10.1007/s002449900454.
[2] J.B. Burkholder, R.A. Cox, A.R. Ravishankara, Atmospheric Degradation of Ozone Depleting Substances, Their Substitutes, and Related Species, Chem. Rev. 115 (10) (2015) 3704–3759, https://doi.org/10.1021/cr5006759.
[3] S.R. Sellevåg, T. Kelly, H. Sidebottom, C.J. Nielsen, A study of the IR and UV-Vis absorption cross-sections, photolysis and OH-initiated oxidation of $CF_3CHO$ and $CF_3CH_2CHO$, Phys. Chem. Chem. Phys. 6 (6) (2004) 1243–1252, https://doi.org/10.1039/B315941H.
[4] C.V. Berney, Spectroscopy of $CF_3COZ$ compounds-III. Vibrational spectrum and barrier to internal rotation of trifluoroacetaldehyde, Spectrochim. Acta Part A Mol, Biomol. Spectrosc. 25 (4) (1969) 793–809, https://doi.org/10.1016/0584-8539(69)80053-x.
[5] J.R. Durig, G.A. Guirgis, B.J. Van Der Veken, Van Der Veken, Raman spectra of gases. XXVI—Trifluoroacetaldehyde, J. Raman Spectrosc. 18 (8) (1987) 549–553, https://doi.org/10.1002/jrs.1250180804.
[6] R.C. Woods, Microwave spectrum, dipole moment, and barrier to internal rotation of fluoral, J. Chem. Phys. 46 (12) (1967) 4789–4799, https://doi.org/10.1063/1.1840637.
[7] I. Kleiner, Asymmetric-top molecules containing one methyl-like internal rotor: Methods and codes for fitting and predicting spectra, J. Mol. Spectrosc. 260 (1) (2010) 1–18, https://doi.org/10.1016/j.jms.2009.12.011.
[8] R.C. Woods, A general program for the calculation of internal rotation splittings in microwave spectroscopy, J. Mol. Spectrosc. 22 (1-4) (1967) 49–59, https://doi.org/10.1016/0022-2852(67)90147-6.
[9] C. Cabezas, J.-C. Guillemin, Y. Endo, Fourier-transform microwave spectroscopy of a halogen substituted Criegee intermediate ClCHOO, J. Chem. Phys. 145 (18) (2016) 184304, https://doi.org/10.1063/1.4967250.
[10] H. Gilman, R.G. Jones, 2,2,2-Trifluoroethylamine and 2,2,2-Trifluorodiazoethane, J. Am. Chem. Soc. 65 (8) (1943) 1458–1460, https://doi.org/10.1021/ja01248a005.
[11] Y. Endo, H. Kohguchi, Y. Ohshima, PDN-FTMW spectroscopy of open-shell complexes, Faraday Discuss. 97 (1994) 341–350, https://doi.org/10.1039/FD9949700341.
[12] Y. Sumiyoshi, H. Katsunuma, K. Suma, Y. Endo, Spectroscopy of Ar–SH and Ar–SD. I. Observation of rotation-vibration transitions of a van der Waals mode by double-resonance spectroscopy, J. Chem. Phys. 123 (5) (2005) 054324, https://doi.org/10.1063/1.1943967.
[13] H. Ogoshi, H. Mizushima, H. Toi, Y. Aoyama, l, l, l-Trifluoro-2-penten-4-one as a Building Block of Trifluoromethyl-Substituted Compounds, J. Org. Chem. 51 (1986) 2366–2368, https://doi.org/10.1021/jo00362a034.
[14] L. Zou, R.A. Motiyenko, L. Margulès, E.A. Alekseev, Millimeter-wave emission spectrometer based on direct digital synthesis, Rev. Sci. Instrum. 91 (6) (2020) 063104, https://doi.org/10.1063/5.0004461.
[15] H. Hartwig, H. Dreizler, The microwave spectrum of trans-2, 3-dimethyloxirane in torsional excited states, Zeitschrift Für Naturforsch. A. 51 (1996) 923–932, https://doi.org/10.1515/zna-1996-0807.
[16] V.V. Ilyushin, Z. Kisiel, L. Pszczólkowski, H. Mäder, J.T. Hougen, A new torsion–rotation fitting program for molecules with a sixfold barrier: Application to the microwave spectrum of toluene, J. Mol. Spectrosc. 259 (1) (2010) 26–38, https://doi.org/10.1016/j.jms.2009.10.005.
[17] V.V. Ilyushin, C.P. Endres, F. Lewen, S. Schlemmer, B.J. Drouin, Submillimeter wave spectrum of acetic acid, J. Mol. Spectrosc. 290 (2013) 31–41, https://doi.org/10.1016/j.jms.2013.06.005.
[18] E. Herbst, J.K. Messer, F.C. De Lucia, P. Helminger, A new analysis and additional measurements of the millimeter and submillimeter spectrum of methanol, J. Mol. Spectrosc. 108 (1) (1984) 42–57, https://doi.org/10.1016/0022-2852(84)90285-6.
[19] J.T. Hougen, I. Kleiner, M. Godefroid, Selection Rules and Intensity Calculations for a Cs Asymmetric Top Molecule Containing a Methyl Group Internal Rotor, J. Mol. Spectrosc. 163 (2) (1994) 559–586, https://doi.org/10.1006/jmsp.1994.1047.
[20] G.M. Plummer, E. Herbst, F.C. De Lucia, C-type transitions in methyl formate, Astrophys. J. 318 (1987) 873–875, https://doi.org/10.1086/165418.
[21] K. Nakagawa, S. Tsunekawa, T. Kojima, Effective torsion-rotation Hamiltonian for methanol-type molecules, J. Mol. Spectrosc. 126 (2) (1987) 329–340, https://doi.org/10.1016/0022-2852(87)90240-2.

[22] M.S. Walsh, L.-H. Xu, R.M. Lees, Global Fit of Torsion-Rotation Transitions in the Ground and First Excited Torsional States of $CD_3OH$ Methanol, J. Mol. Spectrosc. 188 (1) (1998) 85–93, https://doi.org/10.1006/JMSP.1997.7503.
[23] J.L. Alonso, A. Lesarri, J.C. Lopez, S. Blanco, I. Kleiner, J. Demaison, Rotational spectrum, internal rotation barrier and structure of 3,3,3-trifluoropropene, Mol. Phys. 91 (1997) 731–750, https://doi.org/10.1080/002689797171229.
[24] L. Zou, R.A. Motiyenko, L. Margulès, WH11: Accurate torsional barrier height of trifluroacetic acid, 74th Int, Symp. Mol, Spectrosc, 2020, https://www.ideals.illinois.edu/handle/2142/107441.
[25] L.-H. Xu, J. Fisher, R.M. Lees, H.Y. Shi, J.T. Hougen, J.C. Pearson, B.J. Drouin, G.A. Blake, R. Braakman, Torsion–rotation global analysis of the first three torsional states (νt= 0, 1, 2) and terahertz database for methanol, J. Mol. Spectrosc. 251 (1-2) (2008) 305–313, https://doi.org/10.1016/j.jms.2008.03.017.
[26] I.A. Smirnov, E.A. Alekseev, V.V. Ilyushin, L. Margulés, R.A. Motiyenko, B.J. Drouin, Spectroscopy of the ground, first and second excited torsional states of acetaldehyde from 0.05 to 1.6 THz, J. Mol. Spectrosc. 295 (2014) 44–50, https://doi.org/10.1016/j.jms.2013.11.006.
[27] C.C. Lin, J.D. Swalen, Internal Rotation and Microwave Spectroscopy, Rev. Mod. Phys. 31 (1959) 841–892, https://doi.org/10.1103/RevModPhys.31.841.
[28] I. Kleiner, F.J. Lovas, M. Godefroid, Microwave Spectra of Molecules of Astrophysical Interest. XXIII. Acetaldehyde, J. Phys. Chem. Ref. Data. 25 (4) (1996) 1113–1210, https://doi.org/10.1063/1.555983.